

Coincidence detection probability of $(\gamma, 2e)$ photoemission measurement

Yuehua Su,^{1,*} Kun Cao,¹ and Chao Zhang¹

¹ *Department of Physics, Yantai University, Yantai 264005, People's Republic of China*

In the study of the strongly correlated electrons, one of the challenging core tasks is to develop the potential techniques for direct detection of the many-body correlations of the strongly correlated electrons. $(\gamma, 2e)$ photoemission technique has been developed to investigate the two-body correlations of the target correlated electrons. In this article, we will focus on this technique for the correlated electrons near the Fermi energy. The coincidence detection probability of the two emitted electrons in the $(\gamma, 2e)$ photoemission measurement is shown to be relevant to a two-body Bethe-Salpeter wave function, which describes the dynamical two-body correlations of the target correlated electrons. As the coincidence detection probability involves an electron-electron interaction matrix element, the arbitrary momentum and/or energy transfer due to this electron-electron interaction makes the $(\gamma, 2e)$ photoemission technique fail to reveal the inner-pair structure of the two-body Bethe-Salpeter wave function. However, the center-of-mass momentum and energy of the two-body Bethe-Salpeter wave function can be distinctly resolved. Thus, the $(\gamma, 2e)$ photoemission technique can provide the center-of-mass physics of the two-body Bethe-Salpeter wave function of the target correlated electrons. It would be one potential technique to study the center-of-mass physics of the Cooper pairs in superconductor.

I. INTRODUCTION

The most challenge in the field of the strongly correlated electrons is to understand the many-body correlations and the relevant experimental phenomena [1–5]. One core task in this field is to develop the potential techniques for direct detection of the many-body correlations of the strongly correlated electrons. Recently, two coincidence techniques, a coincidence angle-resolved photoemission spectroscopy (cARPES) [6] and a coincidence inelastic neutron scattering (cINS) [7] have been proposed to detect the two-body correlations of the strongly correlated electrons. The cARPES detects the coincidence probability of two photoelectric processes, which can be developed to study the two-body correlations of the target correlated electrons in particle-particle channel. The cINS detects the coincidence probability of two spin scattering processes, which can study the two-spin correlations of the target spin systems. There are two basic principles in the theory of the two proposed coincidence detection techniques: (1) The intrinsic two-body correlations can be directly detected by two-body coincidence detection, and (2) the coincidence detection probability is determined by the second-order perturbations of the interaction between the target matter and the external probe field. These basic principles can be introduced to develop other experimental techniques to study the many-body correlations of the target matter in other channels.

In this article, we will focus on an early proposed coincidence technique, the $(\gamma, 2e)$ photoemission. It is sometimes called double photoemission. The $(\gamma, 2e)$ photoemission technique has been developed to study the core and the Auger electrons [8], the atomic and the molec-

ular electrons [9–11], the valence electrons [12, 13], the surface electrons [14], the Cooper pairs [15], *etc.* In the $(\gamma, 2e)$ photoemission measurement, there are mainly two types of contributions from two sequential microscopic physical processes. In type I photoemission, the two sequential microscopic physical processes involve: (i) One incident photon excites one electron of the target matter into a high-energy intermediate state, and (ii) the excited electron interacts with another electron by an electron-electron interaction which scatters these two electrons outside the target matter in the final state. In type II photoemission, the sequential microscopic physical processes include: (i) One incident photon emits one photoelectron outside the target matter with one hole left, and (ii) two electrons in the target matter interact with each other with one excited to annihilate the left hole and the other scattered outside in the final state. The two emitted electrons are detected coincidentally in the $(\gamma, 2e)$ photoemission measurement, which can provide the information on the two-body correlations of the target-matter electrons.

The theories for the $(\gamma, 2e)$ photoemission technique to study the correlated electrons near the Fermi energy have been developed recently [16–18]. In reference [16], the author utilized the Fermi's golden rule to describe the single-photon absorption process and then introduced the time-reversed evolution technique to define the final state. With this theoretical treatment, the two sequential physical processes in the $(\gamma, 2e)$ photoemission can be included in the coincidence detection probability. The references [17, 18] involve a similar idea in the definition of the coincidence current, where the initial and the final states are introduced with perturbation electron-electron interaction. These theories are too complex in especially their description of the dynamical properties of the two-body correlations of the target electrons. Moreover, as we will show in this article, the coincidence detection probability is determined in principle

*Electronic address: suyh@ytu.edu.cn

by the second-order perturbations of the electron-photon and the electron-electron interactions. Therefore, a well-defined theory for the $(\gamma, 2e)$ photoemission measurement should be a second-order perturbation theory. In the previous theories [16–18], the sequential photon absorption and electron-electron scattering are treated separately, where the former is by the Fermi's golden rule of the first-order perturbation theory and the latter is by the time-reversed evolution technique with electron-electron interaction perturbations. This theoretical treatment seems inaccurate in principle.

In this article, we will develop a second-order perturbation theory for the $(\gamma, 2e)$ photoemission measurement. We will focus on the correlated electrons near the Fermi energy. Physically, the coincidence detection probability in the $(\gamma, 2e)$ photoemission measurement is defined by the coincidence probability of the two sequential microscopic physical processes, (i) one photon absorption and (ii) electron-electron scattering. Mathematically, the coincidence detection probability is determined by the second-order perturbations of the two relevant interactions of the two sequential microscopic physical processes. The coincidence detection probability is shown to be relevant to a dynamical two-body Bethe-Salpeter wave function, which describes the dynamical two-body correlations of the target electrons. As the coincidence detection probability of the $(\gamma, 2e)$ photoemission measurement involves an electron-electron interaction matrix element which has arbitrary momentum and/or energy transfer, the inner-pair structure of the two-body Bethe-Salpeter wave function can not be resolved. Meanwhile, as the center-of-mass momentum and energy of the two-body Bethe-Salpeter wave function can be resolved, the coincidence detection probability of the $(\gamma, 2e)$ photoemission measurement can reveal the center-of-mass physics of the two-body Bethe-Salpeter wave function. Therefore, the $(\gamma, 2e)$ photoemission technique can be introduced to study the center-of-mass physics of the two-body correlations of the target correlated electrons, such as the center-of-mass physics of the Cooper pairs in superconductor.

Our article is arranged as below. In Sec. II, we will develop a second-order perturbation theory for the $(\gamma, 2e)$ photoemission measurement. In Sec. III, we will consider a simple case where the electron-electron interaction in the electron-electron scattering process is a frequency-independent Coulomb interaction. Discussion on the coincidence detection of the Cooper-pair physics by the $(\gamma, 2e)$ photoemission technique is given in Sec. IV, where a simple summary is also presented.

II. THEORY FOR $(\gamma, 2e)$ PHOTOEMISSION MEASUREMENT

In this section, we will present a detailed study to develop a second-order perturbation theory for the $(\gamma, 2e)$ photoemission measurement.

As we have discussed in Sec. I, the $(\gamma, 2e)$ photoemission involves two sequential microscopic physical processes, (i) one photon absorption and (ii) electron-electron scattering. The two relevant interactions of the two microscopic physical processes, the electron-photon interaction V_1 and the electron-electron interaction V_2 , are defined respectively as following:

$$V_1(t) = \sum_{\mathbf{k}\mathbf{q}\lambda\sigma} g_\lambda(\mathbf{k}, \mathbf{q}) d_{\mathbf{k}+\mathbf{q}\sigma}^\dagger(t) c_{\mathbf{k}\sigma}(t) [a_{\mathbf{q}\lambda}(t) + a_{-\mathbf{q}\lambda}^\dagger(t)], \quad (1)$$

and

$$V_2(t_1, t_2) = \frac{1}{2} \sum_{\mathbf{k}_1\mathbf{k}_2\mathbf{q}_1\sigma_1\sigma_2} U(\mathbf{k}_1, \mathbf{k}_2, \mathbf{q}_1; t_1, t_2) f_{\mathbf{k}_1+\mathbf{q}_1\sigma_1}^\dagger(t_1) \times e_{\mathbf{k}_1\sigma_1}(t_1) d_{\mathbf{k}_2-\mathbf{q}_1\sigma_2}^\dagger(t_2) c_{\mathbf{k}_2\sigma_2}(t_2). \quad (2)$$

Here $c_{\mathbf{k}\sigma}(d_{\mathbf{k}\sigma}, e_{\mathbf{k}\sigma}, f_{\mathbf{k}\sigma})$ and $c_{\mathbf{k}\sigma}^\dagger(d_{\mathbf{k}\sigma}^\dagger, e_{\mathbf{k}\sigma}^\dagger, f_{\mathbf{k}\sigma}^\dagger)$ are the annihilation and the creation operators for the electrons with momentum \mathbf{k} and spin σ , $a_{\mathbf{q}\lambda}$ and $a_{\mathbf{q}\lambda}^\dagger$ are the annihilation and the creation operators for the photons with momentum \mathbf{q} and polarization λ . For clarity and brevity, we have introduced the different symbols c, d, e, f for the electrons in the possible different electron bands. The more general forms of the electron-photon and the electron-electron interactions in crystal matter have been presented in Appendix A. The band-index dependence of the interaction matrix elements g and U is not explicitly shown. In general cases, the electron-electron interaction V_2 involves time-retarded dynamics. In the below, we will assume that $U = U(\mathbf{k}_1, \mathbf{k}_2, \mathbf{q}_1; t_1 - t_2)$ which follows the energy conservation. These two interactions are shown schematically in Fig. 1.

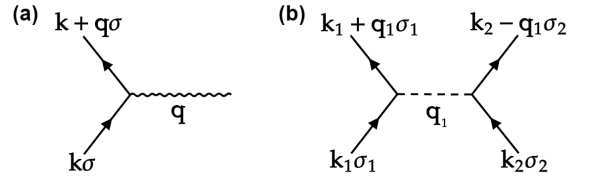


FIG. 1: Two relevant interactions in the $(\gamma, 2e)$ photoemission: (a) Electron-photon interaction V_1 , and (b) electron-electron interaction V_2 .

The Hamiltonian of the combined system of the target electrons and the incident photons is defined by

$$H_T = H + V_1 + V_2, \quad H = H_e + H_p, \quad (3)$$

where H_e is the Hamiltonian of the target electrons, where all of the electron-electron interactions are involved except the ones we have separated out in (2) which are specially relevant to the $(\gamma, 2e)$ photoemission, and H_p is the photon Hamiltonian defined by $H_p = \sum_{\mathbf{q}\lambda} \hbar\omega_{\mathbf{q}}(a_{\mathbf{q}\lambda}^\dagger a_{\mathbf{q}\lambda} + \frac{1}{2})$.

In the below, we will take the two interactions V_1 and V_2 as the perturbation interactions. We can define the S -matrix operator as following:

$$S = T_t e^{-\frac{i}{\hbar} [\int_{-\infty}^{\infty} dt V_1(t) + \int_{-\infty}^{\infty} dt_1 dt_2 V_2(t_1, t_2)]}, \quad (4)$$

where T_t is the time-order operator. Suppose the incident photon has momentum \mathbf{q} and polarization λ , and the two emitted electrons in the final state have momenta and spins $\mathbf{k}_1\sigma_1$ and $\mathbf{k}_2\sigma_2$, respectively. The coincidence detection probability of the two emitted electrons in the $(\gamma, 2e)$ photoemission measurement can be defined by

$$\Gamma = \frac{1}{Z} \sum_{\alpha\beta} e^{-\beta E_\alpha} |\langle \Psi_\beta; \mathbf{k}_1\sigma_1, \mathbf{k}_2\sigma_2 | S^{(2)} | \Psi_\alpha; \mathbf{q}\lambda \rangle|^2, \quad (5)$$

where $|\Psi_\alpha\rangle$ and $|\Psi_\beta\rangle$ are the initial and the final states of the target electrons in the $(\gamma, 2e)$ photoemission measurement, E_α is the corresponding eigenvalue of the initial state $|\Psi_\alpha\rangle$. $S^{(2)}$ is a second-order expansion of the S -matrix,

$$S^{(2)} = \frac{(-i)^2}{2!\hbar^2} \iiint_{-\infty}^{+\infty} dt_1 dt_2 dt_3 T_t [V_2(t_2, t_3) V_1(t_1)]. \quad (6)$$

It should be noted that here we have assumed an initial single-photon state in the definition of the coincidence detection probability Γ . This is just for discussion to be simple. In the realistic experiment, the incident photons can be in the macroscopic coherent state or other multiphoton states. In this case, the coincidence detection probability Γ can be similarly defined with the new initial and final photon states. All of the following results can be obtained with an additional factor to account for the redefined photon states.

In order to describe the coincidence detection probability Γ , following the theoretical treatment for cARPES [6], we introduce a two-body Bethe-Salpeter wave function [19, 20],

$$\Phi_{\alpha\beta}(\mathbf{k}_1\sigma_1, t_1; \mathbf{k}_2\sigma_2, t_2) = \langle \Psi_\beta | T_t c_{\mathbf{k}_1\sigma_1}(t_1) c_{\mathbf{k}_2\sigma_2}(t_2) | \Psi_\alpha \rangle. \quad (7)$$

It describes the physics of the electrons when two of the electrons are annihilated in time ordering. Thus, it describes the dynamical two-body correlations of the electrons in particle-particle channel. Introduce the center-of-mass time $t_c = \frac{1}{2}(t_1 + t_2)$ and the relative time $t_r = t_1 - t_2$, the Bethe-Salpeter wave function can be reexpressed into $\Phi_{\alpha\beta}(\mathbf{k}_1\sigma_1, \mathbf{k}_2\sigma_2; t_c, t_r) = \Phi_{\alpha\beta}(\mathbf{k}_1\sigma_1, t_1; \mathbf{k}_2\sigma_2, t_2)$. The Fourier transformations of the two-body Bethe-Salpeter wave function are defined by

$$\begin{aligned} & \Phi_{\alpha\beta}(\mathbf{k}_1\sigma_1, \mathbf{k}_2\sigma_2; t_c, t_r) \\ &= \iint_{-\infty}^{+\infty} \frac{d\Omega d\omega}{(2\pi)^2} \Phi_{\alpha\beta}(\mathbf{k}_1\sigma_1, \mathbf{k}_2\sigma_2; \Omega, \omega) e^{-i\Omega t_c - i\omega t_r}, \end{aligned} \quad (8)$$

$$\begin{aligned} & \Phi_{\alpha\beta}(\mathbf{k}_1\sigma_1, \mathbf{k}_2\sigma_2; \Omega, \omega) \\ &= \iint_{-\infty}^{+\infty} dt_c dt_r \Phi_{\alpha\beta}(\mathbf{k}_1\sigma_1, \mathbf{k}_2\sigma_2; t_c, t_r) e^{i\Omega t_c + i\omega t_r}. \end{aligned} \quad (9)$$

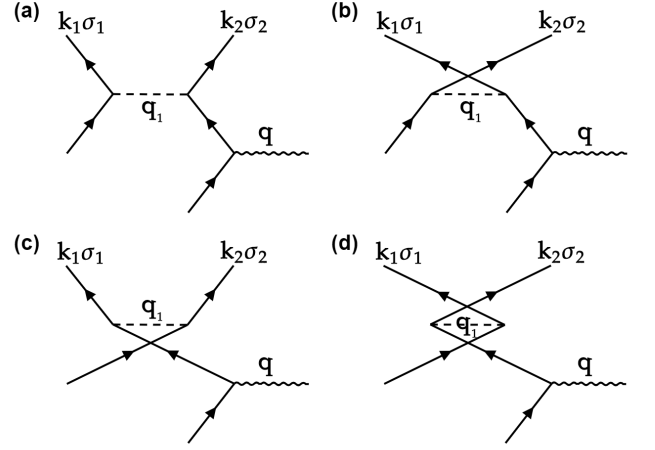


FIG. 2: Schematic illustration of the four contributions $P_{\alpha\beta,i}$ with $i = 1, 2, 3, 4$ to the coincidence detection probability Γ_I in type-I photoemission. Here $i = 1, 2, 3, 4$ correspond to (a), (b), (c) and (d), respectively.

Let us first consider the contributions from type-I photoemission processes. They are schematically shown in Fig. 2. In type-I photoemission, there are two sequential microscopic physical processes involved: (i) One incident photon excites one electron of the target matter into a high-energy intermediate state, and (ii) the excited electron interacts with another electron by the interaction V_2 which scatters these two electrons outside in the final state. The coincidence detection probability of the two emitted electrons from type-I photoemission can be defined by the coincidence probability of the two microscopic physical processes in type-I photoemission, which can be shown to follow

$$\Gamma_I = \frac{1}{Z} \sum_{\alpha\beta} e^{-\beta E_\alpha} \left| \sum_{i=1}^4 P_{\alpha\beta,i} \right|^2, \quad (10)$$

where the four contributions $P_{\alpha\beta,i}$, $i = 1, 2, 3, 4$ to Γ_I are schematically shown in Fig. 2.

A detailed calculation of these four contributions is presented in Appendix B. It can be shown that $P_{\alpha\beta,1} = P_{\alpha\beta,1}(\mathbf{k}_1\sigma_1, \mathbf{k}_2\sigma_2)$ follows

$$\begin{aligned} & P_{\alpha\beta,1}(\mathbf{k}_1\sigma_1, \mathbf{k}_2\sigma_2) \\ &= \frac{-1}{4\hbar^2} \sum_{\mathbf{q}_1} g_\lambda(\mathbf{k}_2 + \mathbf{q}_1 - \mathbf{q}, \mathbf{q}) U(\mathbf{k}_1 - \mathbf{q}_1, \mathbf{k}_2 + \mathbf{q}_1, \mathbf{q}_1; \omega_1) \\ & \quad \times \Phi_{\alpha\beta}(\mathbf{k}_1 - \mathbf{q}_1\sigma_1, \mathbf{k}_2 + \mathbf{q}_1 - \mathbf{q}\sigma_2; \Omega_c, \omega_r), \end{aligned} \quad (11)$$

where the frequencies ω_1 , Ω_c and ω_r are set as

$$\begin{aligned} \omega_1 &= \frac{1}{\hbar} [\varepsilon_{\mathbf{k}_2+\mathbf{q}_1}^{(I)} - \varepsilon_{\mathbf{k}_2}^{(V)}], \\ \Omega_c &= \frac{1}{\hbar} [\varepsilon_{\mathbf{k}_1}^{(V)} + \varepsilon_{\mathbf{k}_2}^{(V)}] - \omega_{\mathbf{q}}, \\ \omega_r &= \frac{1}{2\hbar} [\varepsilon_{\mathbf{k}_1}^{(V)} + \varepsilon_{\mathbf{k}_2}^{(V)}] + \frac{1}{2} \omega_{\mathbf{q}} - \frac{1}{\hbar} \varepsilon_{\mathbf{k}_2+\mathbf{q}_1}^{(I)}. \end{aligned} \quad (12)$$

Here $\omega_{\mathbf{q}}$ is the frequency of the incident photon, $\varepsilon_{\mathbf{k}}^{(I)}$ is the energy of the excited electron in the intermediate state after one photon absorption, and $\varepsilon_{\mathbf{k}}^{(V)}$ is the energy of the emitted electron outside the target matter. $U(\mathbf{k}_1, \mathbf{k}_2, \mathbf{q}_1; \omega_1)$ is the Fourier transformation of $U(\mathbf{k}_1, \mathbf{k}_2, \mathbf{q}; t_1 - t_2)$ as shown in Eq. (B3). It should be noted that here we have made an assumption that the excited electron in the intermediate state can propagate freely in the target matter until it interacts with another electron by the interaction V_2 . This assumption can be a good approximation for the case where the excited electron in the intermediate state has a much higher energy than that of the plasmon excitations. In this case, the excited electron can propagate freely within a very short time so as the plasmon excitations have not been fully excited. Therefore, within this short propagating time, the excited electron has little renormalization effects from the plasmon excitations. Moreover, the sudden approximation [21] is also assumed for the two electrons in the final state, which makes the momenta and energies of these two electrons conserved when they are tunnelling outside the target matter. In the above discussion, the work function has not been considered for simplicity.

The left three contributions $P_{\alpha\beta,2}$, $P_{\alpha\beta,3}$ and $P_{\alpha\beta,4}$ follow the below equalities:

$$P_{\alpha\beta,2}(\mathbf{k}_1\sigma_1, \mathbf{k}_2\sigma_2) = -P_{\alpha\beta,1}(\mathbf{k}_2\sigma_2, \mathbf{k}_1\sigma_1), \quad (13)$$

and

$$\begin{aligned} P_{\alpha\beta,3}(\mathbf{k}_1\sigma_1, \mathbf{k}_2\sigma_2) &= P_{\alpha\beta,2}(\mathbf{k}_1\sigma_1, \mathbf{k}_2\sigma_2), \\ P_{\alpha\beta,4}(\mathbf{k}_1\sigma_1, \mathbf{k}_2\sigma_2) &= P_{\alpha\beta,1}(\mathbf{k}_1\sigma_1, \mathbf{k}_2\sigma_2). \end{aligned} \quad (14)$$

Therefore, the coincidence detection probability of the two emitted electrons in type-I photoemission can be described by

$$\Gamma_{\text{I}} = \frac{4}{Z} \sum_{\alpha\beta} e^{-\beta E_{\alpha}} |P_{\alpha\beta,1}(\mathbf{k}_1\sigma_1, \mathbf{k}_2\sigma_2) - P_{\alpha\beta,1}(\mathbf{k}_2\sigma_2, \mathbf{k}_1\sigma_1)|^2. \quad (15)$$

Now let us study the contributions from type-II photoemission processes. There are four different microscopic contributions as schematically shown in Fig. 3. For each contribution, it involves two sequential microscopic physical processes: (i) One incident photon emits one photoelectron outside the target matter with one hole left, and (ii) two electrons in the target matter interact with each other by the interaction V_2 with one excited to annihilate the left hole and the other scattered outside in the final state. It should be noted that the Auger electron emission [8] can also occur in type-II photoemission if the electrons we considered include the atomic core electrons.

Following a similar calculation to type-I photoemission, we can show that (seen more details in Appendix C)

$$\begin{aligned} P_{\alpha\beta,6}(\mathbf{k}_1\sigma_1, \mathbf{k}_2\sigma_2) &= -P_{\alpha\beta,5}(\mathbf{k}_2\sigma_2, \mathbf{k}_1\sigma_1), \\ P_{\alpha\beta,8}(\mathbf{k}_1\sigma_1, \mathbf{k}_2\sigma_2) &= -P_{\alpha\beta,7}(\mathbf{k}_2\sigma_2, \mathbf{k}_1\sigma_1), \end{aligned} \quad (16)$$

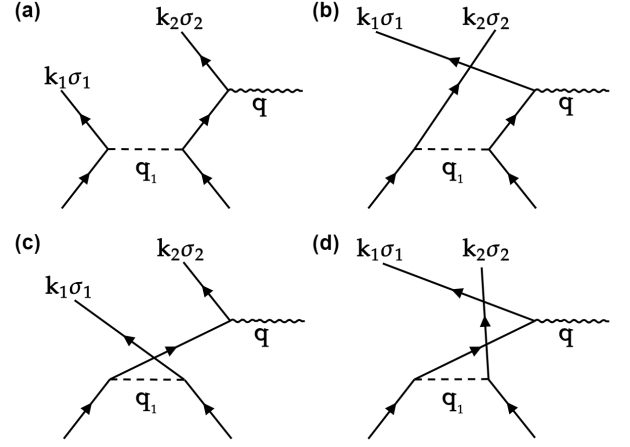


FIG. 3: Schematic illustration of the four contributions $P_{\alpha\beta,i}$, $i = 5, 6, 7, 8$ to the coincidence detection probability Γ_{II} in type-II photoemission. Here $i = 5, 6, 7, 8$ correspond to (a), (b), (c) and (d), respectively.

and $P_{\alpha\beta,5}(\mathbf{k}_1\sigma_1, \mathbf{k}_2\sigma_2)$ and $P_{\alpha\beta,7}(\mathbf{k}_1\sigma_1, \mathbf{k}_2\sigma_2)$ are given in the below:

$$\begin{aligned} P_{\alpha\beta,5}(\mathbf{k}_1\sigma_1, \mathbf{k}_2\sigma_2) &= \frac{1}{4\hbar^2} \sum_{\mathbf{q}_1} \int d\omega_1 g_{\lambda}(\mathbf{k}_2 - \mathbf{q}, \mathbf{q}) U(\bar{\mathbf{k}}_1, \bar{\mathbf{k}}_2, \mathbf{q}_1; \omega_1) \\ &\quad \times \Phi_{\alpha\beta}(\bar{\mathbf{k}}_1\sigma_1, \bar{\mathbf{k}}_2\sigma_2; \Omega_c, \omega_r) \delta(\omega_{\mathbf{q}} - \varepsilon_{\mathbf{k}_2}^{(V)}/\hbar + \varepsilon_{\mathbf{k}_2 - \mathbf{q}}^{(I)}/\hbar), \end{aligned} \quad (17)$$

where $\bar{\mathbf{k}}_1 \equiv \mathbf{k}_1 - \mathbf{q}_1$ and $\bar{\mathbf{k}}_2 \equiv \mathbf{k}_2 + \mathbf{q}_1 - \mathbf{q}$, and the frequencies Ω_c and ω_r are defined as

$$\begin{aligned} \Omega_c &= \frac{1}{\hbar} [\varepsilon_{\mathbf{k}_1}^{(V)} + \varepsilon_{\mathbf{k}_2}^{(V)}] - \omega_{\mathbf{q}}, \\ \omega_r &= \frac{1}{2\hbar} [\varepsilon_{\mathbf{k}_1}^{(V)} - \varepsilon_{\mathbf{k}_2}^{(V)}] + \frac{1}{2} \omega_{\mathbf{q}} - \omega_1. \end{aligned} \quad (18)$$

$$\begin{aligned} P_{\alpha\beta,7}(\mathbf{k}_1\sigma_1, \mathbf{k}_2\sigma_2) &= \frac{-1}{4\hbar^2} \sum_{\mathbf{q}_1} \int d\omega_1 g_{\lambda}(\mathbf{k}_2 - \mathbf{q}, \mathbf{q}) U(\bar{\mathbf{k}}_2, \bar{\mathbf{k}}_1, \mathbf{q}_1; \omega_1) \\ &\quad \times \Phi_{\alpha\beta}(\bar{\mathbf{k}}_2\sigma_2, \bar{\mathbf{k}}_1\sigma_1; \Omega_c, \omega_r) \delta(\omega_{\mathbf{q}} - \varepsilon_{\mathbf{k}_2}^{(V)}/\hbar + \varepsilon_{\mathbf{k}_2 - \mathbf{q}}^{(I)}/\hbar), \end{aligned} \quad (19)$$

where $\bar{\mathbf{k}}_1 \equiv \mathbf{k}_1 + \mathbf{q}_1$ and $\bar{\mathbf{k}}_2 \equiv \mathbf{k}_2 - \mathbf{q}_1 - \mathbf{q}$, and the frequencies Ω_c and ω_r are defined by

$$\begin{aligned} \Omega_c &= \frac{1}{\hbar} [\varepsilon_{\mathbf{k}_1}^{(V)} + \varepsilon_{\mathbf{k}_2}^{(V)}] - \omega_{\mathbf{q}}, \\ \omega_r &= \frac{1}{2\hbar} [\varepsilon_{\mathbf{k}_2}^{(V)} - \varepsilon_{\mathbf{k}_1}^{(V)}] - \frac{1}{2} \omega_{\mathbf{q}} - \omega_1. \end{aligned} \quad (20)$$

The coincidence detection probability contributed from type-II photoemission can be described by

$$\Gamma_{\text{II}} = \frac{1}{Z} \sum_{\alpha\beta} e^{-\beta E_{\alpha}} \left| \sum_{i=5}^8 P_{\alpha\beta,i} \right|^2. \quad (21)$$

In the derivation of the above results for type-II photoemission, we also make assumption that the excited electron after one photon absorption propagates freely within a very short time before it annihilates the left hole. Meanwhile, the sudden approximation [21] is also assumed for the two emitted electrons in type-II photoemission.

The total coincidence detection probability Γ in the $(\gamma, 2e)$ photoemission measurement is defined by

$$\Gamma = \Gamma_I + \Gamma_{II}, \quad (22)$$

where Γ_I and Γ_{II} are given by Eq. (15) and Eq. (21), respectively. Here we have ignored the quantum interference effects of type-I and type-II photoemission processes.

It should be noted that all of the eight contributions to the coincidence detection probability $P_{\alpha\beta,i}$, $i = 1, \dots, 8$, involve an electron-electron interaction matrix element $U(\mathbf{k}_1, \mathbf{k}_2, \mathbf{q}_1; \omega_1)$. This interaction matrix element shows the inter-electron momentum- \mathbf{q}_1 transfer between the two interacting electrons in the electron-electron scattering process of the $(\gamma, 2e)$ photoemission. It leads to a momentum- \mathbf{q}_1 summation for the coincidence detection probability. Moreover, the interaction matrix element also involves the inter-electron energy- ω_1 transfer between the two interacting electrons. While the energy transfer in type-I photoemission is locked by the momenta, the energy transfer in type-II photoemission is freely arbitrary. The arbitrary energy transfer leads to an additional frequency integral in the contributions to the coincidence detection probability from type-II photoemission. The arbitrary momentum and/or energy transfer makes the $(\gamma, 2e)$ photoemission technique fail to reveal the inner-pair spatial and dynamical structure of the two-body Bethe-Salpeter wave function. Thus, the $(\gamma, 2e)$ photoemission technique can not reveal the inner-pair physics of the two-body correlations of the target electrons.

Although there are arbitrary inter-electron momentum and energy transfers between the two interacting electrons in the V_2 driven electron-electron scattering process, the center-of-mass momentum and energy of the two interacting electrons are conserved. This makes the center-of-mass momentum and energy of the two-body Bethe-Salpeter wave function to be resolved in the $(\gamma, 2e)$ photoemission measurement. Thus, the coincidence detection probability of the $(\gamma, 2e)$ photoemission measurement can provide the center-of-mass physics of the two-body correlations of the target electrons, with the electron-photon and the electron-electron interaction matrix elements g and U being the renormalization matrix elements. Therefore, the $(\gamma, 2e)$ photoemission technique can be introduced to study the center-of-mass physics of the two-body correlations of the target electrons, *e.g.*, the center-of-mass physics of the Cooper pairs in superconductor. It should be remarked that the proposed cARPES can provide both the inner-pair and the center-of-mass physics of the two-body correlations of the

target electrons [6].

III. SIMPLIFICATION: WITH INSTANTANEOUS COULOMB INTERACTION

Let us consider a simplified case, where the electron-electron interaction V_2 in the electron-electron scattering process of the $(\gamma, 2e)$ photoemission is the instantaneous Coulomb interaction without time-retarded frequency dependence. This is an assumption for the case where the electron-electron scattering process has much smaller time scale than that of the renormalization physical processes, such as the charge density plasmon fluctuations. In this case, the electron-electron scattering process occurs within a much short time so as the left charged particles, the charged ions and the other electrons, have not enough time to response this scattering process. Thus, the relevant electron-electron interaction V_2 can be instantaneous without time-retarded dynamics. This is reasonable for type-I photoemission, where one of the two interacting electrons of the interaction V_2 is the excited electron in a high-energy intermediate state. For type-II photoemission, this is also reasonable if the created hole by the one photon absorption has a much lower energy than the energy scales of the renormalization physical processes. For the other cases, the time-retarded renormalization effects should be included in the electron-electron interaction V_2 .

The instantaneous electron-electron interaction V_2 can be defined as

$$V_2(t) = \frac{1}{2} \sum_{\mathbf{k}_1 \mathbf{k}_2 \mathbf{q}_1 \sigma_1 \sigma_2} U(\mathbf{q}_1) f_{\mathbf{k}_1 + \mathbf{q}_1 \sigma_1}^\dagger(t) e_{\mathbf{k}_2 - \mathbf{q}_1 \sigma_2}^\dagger(t) \times d_{\mathbf{k}_2 \sigma_2}(t) c_{\mathbf{k}_1 \sigma_1}(t). \quad (23)$$

A general form of $U(\mathbf{q}_1)$ can be obtained with the same method provided in Appendix A. For the electrons in plane-wave states, the electron-electron instantaneous Coulomb interaction follows

$$U(\mathbf{q}_1) = \frac{e^2}{\varepsilon_0 V_D (|\mathbf{q}_1|^2 + q_\lambda^2)}, \quad (24)$$

where ε_0 is the permittivity of vacuum, V_D is the system volume. Here $1/q_\lambda$ defines the screened length which comes from the spatial renormalization of the charged particles in the matter.

With a similar calculation to Appendix B, we can show that in the case with the instantaneous electron-electron interaction V_2 , $P_{\alpha\beta,i}$, $i = 1, 2, 3, 4$ from type-I photoemission also follow Eq. (13) and (14), and

$$\begin{aligned} & P_{\alpha\beta,1}(\mathbf{k}_1 \sigma_1, \mathbf{k}_2 \sigma_2) \\ &= \frac{-1}{4\hbar^2} \sum_{\mathbf{q}_1} g_\lambda(\mathbf{k}_2 + \mathbf{q}_1 - \mathbf{q}, \mathbf{q}) U(\mathbf{q}_1) \\ & \times \Phi_{\alpha\beta}(\mathbf{k}_1 - \mathbf{q}_1 \sigma_1, \mathbf{k}_2 + \mathbf{q}_1 - \mathbf{q} \sigma_2; \Omega_c, \omega_r), \quad (25) \end{aligned}$$

where the frequencies Ω_c and ω_r are defined by

$$\begin{aligned}\Omega_c &= \frac{1}{\hbar}[\varepsilon_{\mathbf{k}_1}^{(V)} + \varepsilon_{\mathbf{k}_2}^{(V)}] - \omega_{\mathbf{q}}, \\ \omega_r &= \frac{1}{2\hbar}[\varepsilon_{\mathbf{k}_1}^{(V)} + \varepsilon_{\mathbf{k}_2}^{(V)}] + \frac{1}{2}\omega_{\mathbf{q}} - \frac{1}{\hbar}\varepsilon_{\mathbf{k}_2+\mathbf{q}_1}^{(I)}.\end{aligned}\quad (26)$$

For type-II photoemission, we can show that in this case, $P_{\alpha\beta,5}(\mathbf{k}_1\sigma_1, \mathbf{k}_2\sigma_2)$ and $P_{\alpha\beta,7}(\mathbf{k}_1\sigma_1, \mathbf{k}_2\sigma_2)$ follow as below:

$$\begin{aligned}&P_{\alpha\beta,5}(\mathbf{k}_1\sigma_1, \mathbf{k}_2\sigma_2) \\ &= \frac{\pi}{2\hbar^2} \sum_{\mathbf{q}_1} g_{\lambda}(\mathbf{k}_2 - \mathbf{q}, \mathbf{q}) U(\mathbf{q}_1) \Phi_{\alpha\beta}(\bar{\mathbf{k}}_1\sigma_1, \bar{\mathbf{k}}_2\sigma_2; \Omega_c) \\ &\quad \times \delta(\omega_{\mathbf{q}} - \varepsilon_{\mathbf{k}_2}^{(V)}/\hbar + \varepsilon_{\mathbf{k}_2-\mathbf{q}}^{(I)}/\hbar),\end{aligned}\quad (27)$$

where $\bar{\mathbf{k}}_1 \equiv \mathbf{k}_1 - \mathbf{q}_1$ and $\bar{\mathbf{k}}_2 \equiv \mathbf{k}_2 + \mathbf{q}_1 - \mathbf{q}$, and the frequencies Ω_c is defined as

$$\Omega_c = \frac{1}{\hbar}[\varepsilon_{\mathbf{k}_1}^{(V)} + \varepsilon_{\mathbf{k}_2}^{(V)}] - \omega_{\mathbf{q}}, \quad (28)$$

and

$$\begin{aligned}&P_{\alpha\beta,7}(\mathbf{k}_1\sigma_1, \mathbf{k}_2\sigma_2) \\ &= \frac{-\pi}{2\hbar^2} \sum_{\mathbf{q}_1} g_{\lambda}(\mathbf{k}_2 - \mathbf{q}, \mathbf{q}) U(\mathbf{q}_1) \Phi_{\alpha\beta}(\bar{\mathbf{k}}_2\sigma_2, \bar{\mathbf{k}}_1\sigma_1; \Omega_c) \\ &\quad \times \delta(\omega_{\mathbf{q}} - \varepsilon_{\mathbf{k}_2}^{(V)}/\hbar + \varepsilon_{\mathbf{k}_2-\mathbf{q}}^{(I)}/\hbar),\end{aligned}\quad (29)$$

where $\bar{\mathbf{k}}_1 \equiv \mathbf{k}_1 + \mathbf{q}_1$ and $\bar{\mathbf{k}}_2 \equiv \mathbf{k}_2 - \mathbf{q}_1 - \mathbf{q}$, and Ω_c is also defined by Eq. (28). Here $\Phi_{\alpha\beta}(\mathbf{k}_1\sigma_1, \mathbf{k}_2\sigma_2; \Omega_c) \equiv \Phi_{\alpha\beta}(\mathbf{k}_1\sigma_1, \mathbf{k}_2\sigma_2; \Omega_c, t_r = 0)$. Moreover, it can be shown that the equalities in Eq. (16) are also satisfied. The coincidence detection probability of the $(\gamma, 2e)$ photoemission measurement can also be similarly defined by Eqs. (15), (21) and (22).

IV. DISCUSSION AND SUMMARY

In the above sections, we have developed a second-order perturbation theory for the $(\gamma, 2e)$ photoemission measurement. The coincidence detection probability of the two emitted electrons is relevant to a dynamical two-body Bethe-Salpeter wave function. The dynamical two-body Bethe-Salpeter wave function has a general form [6]:

$$\begin{aligned}\Phi_{\alpha\beta}(\mathbf{k}_1\sigma_1, \mathbf{k}_2\sigma_2; \Omega, \omega) &= 2\pi\delta[\Omega + (E_{\beta} - E_{\alpha})/\hbar] \\ &\quad \times \phi_{\alpha\beta}(\mathbf{k}_1\sigma_1, \mathbf{k}_2\sigma_2; \omega),\end{aligned}\quad (30)$$

where $\Phi_{\alpha\beta}(\mathbf{k}_1\sigma_1, \mathbf{k}_2\sigma_2; \omega)$ follows

$$\begin{aligned}&\Phi_{\alpha\beta}(\mathbf{k}_1\sigma_1, \mathbf{k}_2\sigma_2; \omega) \\ &= \sum_{\gamma} \left[\frac{i\langle\Psi_{\beta}|c_{\mathbf{k}_1\sigma_1}|\Psi_{\gamma}\rangle\langle\Psi_{\gamma}|c_{\mathbf{k}_2\sigma_2}|\Psi_{\alpha}\rangle}{\omega + i\delta^+ + (E_{\alpha} + E_{\beta} - 2E_{\gamma})/2\hbar} \right. \\ &\quad \left. + \frac{i\langle\Psi_{\beta}|c_{\mathbf{k}_2\sigma_2}|\Psi_{\gamma}\rangle\langle\Psi_{\gamma}|c_{\mathbf{k}_1\sigma_1}|\Psi_{\alpha}\rangle}{\omega - i\delta^+ - (E_{\alpha} + E_{\beta} - 2E_{\gamma})/2\hbar} \right].\end{aligned}\quad (31)$$

It involves the following physics: (1) The center-of-mass dynamical physics described by the δ -function, $\delta[\Omega + (E_{\beta} - E_{\alpha})/\hbar]$, which shows the energy transfer conservation in the center-of-mass channel. (2) The inner-pair dynamical physics described by $\Phi_{\alpha\beta}(\mathbf{k}_1\sigma_1, \mathbf{k}_2\sigma_2; \omega)$, which shows the propagator-like resonance structures, peaked at $\omega = \pm(E_{\alpha} + E_{\beta} - 2E_{\gamma})/2\hbar$ with the weights defined by $\langle\Psi_{\beta}|c_{\mathbf{k}_1\sigma_1}|\Psi_{\gamma}\rangle\langle\Psi_{\gamma}|c_{\mathbf{k}_2\sigma_2}|\Psi_{\alpha}\rangle$ and $\langle\Psi_{\beta}|c_{\mathbf{k}_2\sigma_2}|\Psi_{\gamma}\rangle\langle\Psi_{\gamma}|c_{\mathbf{k}_1\sigma_1}|\Psi_{\alpha}\rangle$.

As we have discussed in Sec. II, the $(\gamma, 2e)$ photoemission technique fails to reveal the inner-pair structure of the two-body Bethe-Salpeter wave function due to the arbitrary momentum and/or energy transfer in the electron-electron scattering process in the $(\gamma, 2e)$ photoemission. Since the center-of-mass momentum and energy of the dynamical two-body Bethe-Salpeter wave function can be resolved, the $(\gamma, 2e)$ photoemission technique can be used to study the center-of-mass physics of the two-body correlations of the target electrons. As the Cooper pairs stem from the two-body correlations of the correlated electrons in superconductor, the $(\gamma, 2e)$ photoemission technique would be one potential technique to investigate the center-of-mass physics of the Cooper pairs in superconductor.

Let us consider a spin-singlet superconductor. For the dynamical two-body Bethe-Salpeter wave function in $P_{\alpha\beta,1}$ of Eq. (11), $\Phi_{\alpha\beta}(\mathbf{k}_1 - \mathbf{q}_1\sigma_1, \mathbf{k}_2 + \mathbf{q}_1 - \mathbf{q}\sigma_2; \Omega_c, \omega_r)$, the Cooper pairs with the center-of-mass momentum \mathbf{q}_c and frequency Ω_c lead to the following constraints:

$$\begin{aligned}\mathbf{q}_c &= \mathbf{k}_1 + \mathbf{k}_2 - \mathbf{q}, \\ \Omega_c &= \frac{1}{\hbar}[\varepsilon_{\mathbf{k}_1}^{(V)} + \varepsilon_{\mathbf{k}_2}^{(V)}] - \omega_{\mathbf{q}}, \\ \sigma_1 &=\uparrow, \sigma_2=\downarrow.\end{aligned}\quad (32)$$

The other dynamical two-body Bethe-Salpeter wave functions in the contributions of $P_{\alpha\beta,i}$, $i = 2, \dots, 8$ also follow the same constraints. These constraints are defined for the study of the Cooper pairs with the center-of-mass momentum \mathbf{q}_c and frequency Ω_c by the $(\gamma, 2e)$ photoemission measurement where the two emitted electrons have fixed momenta and spins $\mathbf{k}_1\sigma_1$ and $\mathbf{k}_2\sigma_2$, respectively.

Physically, there are two types of excitations of the pairing gap field for the macroscopic superconducting condensate of the superconductor. One is the Goldstone phase mode of the pairing gap field and the other is the Higgs amplitude mode. With the electromagnetic gauge field included, the Goldstone phase mode is modified into the plasmon mode by the so-called Anderson-Higgs mechanism [22, 23]. The plasmon mode is generally gapped with a large gap about $\hbar\omega_p \simeq 10\text{eV}$ in most three-dimensional metallic superconductors. The Higgs amplitude mode is also gapped with a gap value about two times of the Bogoliubov quasiparticle gap [24, 25]. The $(\gamma, 2e)$ photoemission technique can be introduced to study these two types of excitations of the macroscopic superconducting condensate.

In summary, we have developed a second-order perturbation theory for the $(\gamma, 2e)$ photoemission measurement. The coincidence detection probability of the two emitted electrons is relevant to a dynamical two-body Bethe-Salpeter wave function, which describes the dynamical two-body correlations of the target correlated electrons. Due to the arbitrary momentum and/or energy transfer in the electron-electron scattering process of the $(\gamma, 2e)$ photoemission, only the center-of-mass momentum and energy of the dynamical two-body Bethe-Salpeter wave function can be resolved. Therefore, the $(\gamma, 2e)$ photoemission technique would be one potential technique to study the center-of-mass physics of the two-body correlations of the target correlated electrons, such as the

center-of-mass physics of the Cooper pairs in superconductor.

ACKNOWLEDGMENTS

We thank Prof. Jun Chang, Prof. Tao Li and Prof. Shan Qiao for invaluable discussions. This work was supported by the National Natural Science Foundation of China (Grants No. 11774299 and No. 11874318) and the Natural Science Foundation of Shandong Province (Grant No. ZR2023MA015).

Appendix A: Electron-photon and electron-electron interactions in crystal matter

We will present the general second quantization forms of the electron-photon and the electron-electron interactions for the electrons in crystal matter. Let us first consider the electron-photon interaction, which origins from the gauge invariant Hamiltonian $H = \frac{1}{2m}(\mathbf{P} + e\mathbf{A})^2$, where the charge of electron $q_e = -e$ has been included. Expand this Hamiltonian to linear- \mathbf{A} terms and introduce the Coulomb gauge $\nabla \cdot \mathbf{A} = 0$, the electron- \mathbf{A} interaction can be expressed as $V_1 = \frac{e}{m}\mathbf{A} \cdot \mathbf{P}$. Here we ignore the quadratic \mathbf{A}^2 term as it is little relevant to the $(\gamma, 2e)$ photoemission. The second quantization of the electron-photon interaction can be obtained as following:

$$V_1(t) = \sum_{\sigma} \int d\mathbf{r} \Psi_{\sigma}^{\dagger}(\mathbf{r}, t) \left[\frac{e}{m} \mathbf{A}(t) \cdot \mathbf{P} \right] \Psi_{\sigma}(\mathbf{r}, t). \quad (\text{A1})$$

where $\Psi_{\sigma}(\mathbf{r}, t)$ and $\Psi_{\sigma}^{\dagger}(\mathbf{r}, t)$ are the electron annihilation and creation field operators, respectively. $\Psi_{\sigma}(\mathbf{r}, t)$ can be expanded by the Bloch-band electron wave functions $\psi_n(\mathbf{k}, \mathbf{r})$,

$$\Psi_{\sigma}(\mathbf{r}, t) = \sum_{n\mathbf{k}} \psi_n(\mathbf{k}, \mathbf{r}) c_{n\mathbf{k}\sigma}(t), \quad (\text{A2})$$

where n is the band index number and $c_{n\mathbf{k}\sigma}$ is the electron annihilation operator. Here we have ignored the spin-orbit coupling effects on the Bloch-band electron wave functions and the momentum \mathbf{k} is defined within the first Brillouin zone. From the Bloch theorem, we have

$$\psi_n(\mathbf{k}, \mathbf{r}) = \frac{1}{\sqrt{N\Omega_0}} \sum_{\mathbf{G}} a_n(\mathbf{k} + \mathbf{G}) e^{i(\mathbf{k} + \mathbf{G}) \cdot \mathbf{r}}, \quad (\text{A3})$$

where \mathbf{G} is the reciprocal lattice vector, N is the lattice number, and Ω_0 is the unit cell volume. Introduce the Fourier transformation of \mathbf{A} field [26],

$$\mathbf{A}(\mathbf{r}, t) = \sum_{\mathbf{q}\lambda} \sqrt{\frac{\hbar}{2\varepsilon_0\omega_{\mathbf{q}}V_0}} \mathbf{e}_{\lambda}(\mathbf{q}) [a_{\mathbf{q}\lambda}(t) + a_{-\mathbf{q}\lambda}^{\dagger}(t)] e^{i\mathbf{q} \cdot \mathbf{r}}, \quad (\text{A4})$$

where ε_0 is the permittivity of vacuum, $\omega_{\mathbf{q}}$ is the photon frequency, V_0 is the volume for \mathbf{A} field to be enclosed, \mathbf{e}_{λ} is the λ -th polarization unit vector, $a_{\mathbf{q}\lambda}$ and $a_{\mathbf{q}\lambda}^{\dagger}$ are the photon annihilation and creation operators. From Eqs. (A2), (A3) and (A4), the electron-photon interaction in the crystal matter can be expressed into the following form:

$$V_1(t) = \sum_{n_1 n_2 \lambda} \sum_{\mathbf{k} \mathbf{q} \sigma} g_{n_1 n_2 \lambda}(\mathbf{k}, \mathbf{q}) c_{n_1 \mathbf{k} + \mathbf{q} + \mathbf{G} \sigma}^{\dagger}(t) c_{n_2 \mathbf{k} \sigma}(t) [a_{\mathbf{q}\lambda}(t) + a_{-\mathbf{q}\lambda}^{\dagger}(t)], \quad (\text{A5})$$

where $g_{n_1 n_2 \lambda}(\mathbf{k}, \mathbf{q})$ is defined by

$$g_{n_1 n_2 \lambda}(\mathbf{k}, \mathbf{q}) = \sqrt{\frac{e^2 \hbar^3}{2m^2 \varepsilon_0 \omega_{\mathbf{q}} V_0}} \sum_{\mathbf{G}_l} [\mathbf{e}_{\lambda}(\mathbf{q}) \cdot (\mathbf{k} + \mathbf{G}_l)] a_{n_1}^*(\mathbf{k} + \mathbf{q} + \mathbf{G}_l) a_{n_2}(\mathbf{k} + \mathbf{G}_l). \quad (\text{A6})$$

In Eq. (A5), the reciprocal lattice vector \mathbf{G} is defined so as for given \mathbf{k} and \mathbf{q} with \mathbf{k} in the first Brillouin zone, $\mathbf{k} + \mathbf{q} + \mathbf{G}$ is also in the first Brillouin zone.

Now let us consider the electron-electron interaction which follows

$$V_2(t) = \frac{1}{2} \sum_{\sigma_1 \sigma_2} \iint d\mathbf{r}_1 d\mathbf{r}_2 \Psi_{\sigma_1}^\dagger(\mathbf{r}_1, t) \Psi_{\sigma_2}^\dagger(\mathbf{r}_2, t) U(\mathbf{r}_1 - \mathbf{r}_2) \Psi_{\sigma_2}(\mathbf{r}_2, t) \Psi_{\sigma_1}(\mathbf{r}_1, t). \quad (\text{A7})$$

With the electron fields expanded by the Bloch-band electron wave functions as Eq. (A2), we can obtain the second quantization of the electron-electron interaction V_2 in the below form:

$$V_2 = \frac{1}{2} \sum_{n_1 n_2 n_3 n_4} \sum_{\mathbf{k}_1 \mathbf{k}_2 \mathbf{q} \sigma_1 \sigma_2} U_{n_1 n_2 n_3 n_4}(\mathbf{k}_1, \mathbf{k}_2, \mathbf{q}) c_{n_1 \mathbf{k}_1 + \mathbf{q} + \mathbf{G}_1 \sigma_1}^\dagger(t) c_{n_2 \mathbf{k}_2 - \mathbf{q} + \mathbf{G}_2 \sigma_2}^\dagger(t) c_{n_3 \mathbf{k}_2 \sigma_2}(t) c_{n_4 \mathbf{k}_1 \sigma_1}(t), \quad (\text{A8})$$

where $U_{n_1 n_2 n_3 n_4}(\mathbf{k}_1, \mathbf{k}_2, \mathbf{q})$ is defined by

$$U_{n_1 n_2 n_3 n_4}(\mathbf{k}_1, \mathbf{k}_2, \mathbf{q}) = \sum_{\mathbf{G}_l \mathbf{G}_m} U(\mathbf{q}) a_{n_1}^*(\mathbf{k}_1 + \mathbf{q} + \mathbf{G}_l) a_{n_2}^*(\mathbf{k}_2 - \mathbf{q} + \mathbf{G}_m) a_{n_3}(\mathbf{k}_2 + \mathbf{G}_m) a_{n_4}(\mathbf{k}_1 + \mathbf{G}_l). \quad (\text{A9})$$

Here \mathbf{G}_1 and \mathbf{G}_2 in Eq. (A8) are two reciprocal lattice vectors which make $\mathbf{k}_1 + \mathbf{q} + \mathbf{G}_1$ and $\mathbf{k}_2 - \mathbf{q} + \mathbf{G}_2$ to be in the first Brillouin zone, respectively. During the derivation, we have introduced the Fourier transformation of $U(\mathbf{r})$, $U(\mathbf{r}) = \sum_{\mathbf{q}} U(\mathbf{q}) e^{i\mathbf{q} \cdot \mathbf{r}}$.

Appendix B: Calculation of $P_{\alpha\beta,i}, i = 1, 2, 3, 4$ in type-I photoemission

In this Appendix section, we will present a detailed study on $P_{\alpha\beta,i}, i = 1, 2, 3, 4$ in type-I photoemission. They are schematically shown in Fig. 2.

Let us first consider $P_{\alpha\beta,1}$. It can be calculated as following.

$$\begin{aligned} P_{\alpha\beta,1} &= \frac{(-i)^2}{2! \hbar^2} \iiint_{-\infty}^{+\infty} dt_1 dt_2 dt_3 \sum_{\mathbf{k}'_1 \mathbf{k}'_2 \mathbf{q}'_1 \sigma'_1 \sigma'_2} \sum_{\mathbf{k}' \mathbf{q}' \lambda' \sigma'} \frac{1}{2} U(\mathbf{k}'_1, \mathbf{k}'_2, \mathbf{q}'_1; t_2, t_3) g_{\lambda'}(\mathbf{k}', \mathbf{q}') \\ &\quad \times \langle \Psi_\beta; \mathbf{k}_1 \sigma_1, \mathbf{k}_2 \sigma_2 | T_t f_{\mathbf{k}'_1 + \mathbf{q}'_1 \sigma'_1}^\dagger(t_2) c_{\mathbf{k}'_1 \sigma'_1}(t_2) f_{\mathbf{k}'_2 - \mathbf{q}'_2 \sigma'_2}^\dagger(t_3) d_{\mathbf{k}'_2 \sigma'_2}(t_3) d_{\mathbf{k}' + \mathbf{q}' \sigma'}^\dagger(t_1) c_{\mathbf{k}' \sigma'}(t_1) [a_{\mathbf{q}' \lambda'}^\dagger(t_1) + a_{-\mathbf{q}' \lambda'}^\dagger(t_1)] | \Psi_\alpha; \mathbf{q} \lambda \rangle \\ &= \frac{-1}{4 \hbar^2} \iiint_{-\infty}^{+\infty} dt_1 dt_2 dt_3 \sum_{\mathbf{k}'_1 \mathbf{k}'_2 \mathbf{q}'_1 \sigma'_1 \sigma'_2} \sum_{\mathbf{k}' \sigma'} U(\mathbf{k}'_1, \mathbf{k}'_2, \mathbf{q}'_1; t_2, t_3) g_\lambda(\mathbf{k}', \mathbf{q}) e^{-i\omega_{\mathbf{q}} t_1 + i\varepsilon_{\mathbf{k}'_1 + \mathbf{q}'_1}^{(V)} t_2 / \hbar + i\varepsilon_{\mathbf{k}'_2 - \mathbf{q}'_1}^{(V)} t_3 / \hbar} \\ &\quad \times \langle \Psi_\beta | T_t c_{\mathbf{k}'_1 \sigma'_1}(t_2) d_{\mathbf{k}'_2 \sigma'_2}(t_3) d_{\mathbf{k}' + \mathbf{q} \sigma'}^\dagger(t_1) c_{\mathbf{k}' \sigma'}(t_1) | \Psi_\alpha \rangle \delta_{\mathbf{k}_1, \mathbf{k}' + \mathbf{q}'_1} \delta_{\sigma_1 \sigma'_1} \delta_{\mathbf{k}_2, \mathbf{k}'_2 - \mathbf{q}'_1} \delta_{\sigma_2 \sigma'_2} \\ &= \frac{-1}{4 \hbar^2} \iiint_{-\infty}^{+\infty} dt_1 dt_2 dt_3 \sum_{\mathbf{k}'_1 \mathbf{k}'_2 \mathbf{q}'_1 \sigma'_1 \sigma'_2} \sum_{\mathbf{k}' \sigma'} U(\mathbf{k}'_1, \mathbf{k}'_2, \mathbf{q}'_1; t_2, t_3) g_\lambda(\mathbf{k}', \mathbf{q}) e^{-i\omega_{\mathbf{q}} t_1 + i\varepsilon_{\mathbf{k}'_1 + \mathbf{q}'_1}^{(V)} t_2 / \hbar + i\varepsilon_{\mathbf{k}'_2 - \mathbf{q}'_1}^{(V)} t_3 / \hbar} \\ &\quad \times \langle \Psi_\beta | T_t c_{\mathbf{k}'_1 \sigma'_1}(t_2) c_{\mathbf{k}' \sigma'}(t_1) | \Psi_\alpha \rangle \delta_{\mathbf{k}_1, \mathbf{k}' + \mathbf{q}'_1} \delta_{\sigma_1 \sigma'_1} \delta_{\mathbf{k}_2, \mathbf{k}'_2 - \mathbf{q}'_1} \delta_{\sigma_2 \sigma'_2} \delta_{\mathbf{k}'_2, \mathbf{k}' + \mathbf{q}} \delta_{\sigma'_2 \sigma'} e^{-i\varepsilon_{\mathbf{k}'_2}^{(I)} (t_3 - t_1) / \hbar}. \end{aligned} \quad (\text{B1})$$

Here the contraction operations, unlike the common definition for the Green's functions in the many-body perturbation theory, describe the creation-and-annihilation relations. In the second step, the electron emitted outside the target matter with momentum \mathbf{k} and spin σ is assumed to have energy $\varepsilon_{\mathbf{k}}^{(V)}$, and $a_{\mathbf{q}\lambda}(t) = a_{\mathbf{q}\lambda} e^{-i\omega_{\mathbf{q}} t}$ is used where $\omega_{\mathbf{q}}$ is the photon frequency. In the last step, we assume that the electron in the intermediate state excited by the incident photon can propagate freely in the target matter with energy $\varepsilon_{\mathbf{k}'_2}^{(I)}$, thus we have

$$\overline{d_{\mathbf{k}'_2 \sigma'_2}(t_3) d_{\mathbf{k}' + \mathbf{q} \sigma'}^\dagger(t_1)} = \delta_{\mathbf{k}'_2, \mathbf{k}' + \mathbf{q}} \delta_{\sigma'_2 \sigma'} e^{-i\varepsilon_{\mathbf{k}'_2}^{(I)} (t_3 - t_1) / \hbar}. \quad (\text{B2})$$

This is one approximate assumption in our theory for the coincidence detection probability in the $(\gamma, 2e)$ photoemission measurement. Introduce the Fourier transformation of U ,

$$U(\mathbf{k}'_1, \mathbf{k}'_2, \mathbf{q}'_1; t_2, t_3) = \frac{1}{2\pi} \int d\omega_1 U(\mathbf{k}'_1, \mathbf{k}'_2, \mathbf{q}'_1; \omega_1) e^{-i\omega_1 (t_2 - t_3)}. \quad (\text{B3})$$

Note that there is one symmetry for U : $U(\mathbf{k}'_1, \mathbf{k}'_2, \mathbf{q}'_1; t_2 - t_3) = U(\mathbf{k}'_2, \mathbf{k}'_1, -\mathbf{q}'_1; t_3 - t_2)$. With the two-body Bethe-Salpeter wave function defined in Eq. (7) and its Fourier transformations in Eqs. (8) and (9), we can show that $P_{\alpha\beta,1}$ follows Eq. (11).

The definitions of $P_{\alpha\beta,2}$, $P_{\alpha\beta,3}$ and $P_{\alpha\beta,4}$ are given as below:

$$\begin{aligned}
P_{\alpha\beta,2} &= \frac{(-i)^2}{2!\hbar^2} \iiint_{-\infty}^{+\infty} dt_1 dt_2 dt_3 \sum_{\mathbf{k}'_1 \mathbf{k}'_2 \mathbf{q}'_1 \sigma'_1 \sigma'_2} \sum_{\mathbf{k}' \mathbf{q}' \lambda' \sigma'} \frac{1}{2} U(\mathbf{k}'_1, \mathbf{k}'_2, \mathbf{q}'_1; t_2, t_3) g_{\lambda'}(\mathbf{k}', \mathbf{q}') \\
&\quad \times \langle \Psi_\beta; \mathbf{k}_1 \sigma_1, \mathbf{k}_2 \sigma_2 | T_t f_{\mathbf{k}'_1 + \mathbf{q}'_1 \sigma'_1}^\dagger(t_2) c_{\mathbf{k}'_1 \sigma'_1}(t_2) f_{\mathbf{k}'_2 - \mathbf{q}'_1 \sigma'_2}^\dagger(t_3) d_{\mathbf{k}'_2 \sigma'_2}(t_3) d_{\mathbf{k}' + \mathbf{q}' \sigma'}^\dagger(t_1) c_{\mathbf{k}' \sigma'}(t_1) [a_{\mathbf{q}' \lambda'}(t_1) + a_{-\mathbf{q}' \lambda'}^\dagger(t_1)] | \Psi_\alpha; \mathbf{q} \lambda \rangle \\
P_{\alpha\beta,3} &= \frac{(-i)^2}{2!\hbar^2} \iiint_{-\infty}^{+\infty} dt_1 dt_2 dt_3 \sum_{\mathbf{k}'_1 \mathbf{k}'_2 \mathbf{q}'_1 \sigma'_1 \sigma'_2} \sum_{\mathbf{k}' \mathbf{q}' \lambda' \sigma'} \frac{1}{2} U(\mathbf{k}'_1, \mathbf{k}'_2, \mathbf{q}'_1; t_2, t_3) g_{\lambda'}(\mathbf{k}', \mathbf{q}') \\
&\quad \times \langle \Psi_\beta; \mathbf{k}_1 \sigma_1, \mathbf{k}_2 \sigma_2 | T_t f_{\mathbf{k}'_1 + \mathbf{q}'_1 \sigma'_1}^\dagger(t_2) d_{\mathbf{k}'_1 \sigma'_1}(t_2) f_{\mathbf{k}'_2 - \mathbf{q}'_1 \sigma'_2}^\dagger(t_3) c_{\mathbf{k}'_2 \sigma'_2}(t_3) d_{\mathbf{k}' + \mathbf{q}' \sigma'}^\dagger(t_1) c_{\mathbf{k}' \sigma'}(t_1) [a_{\mathbf{q}' \lambda'}(t_1) + a_{-\mathbf{q}' \lambda'}^\dagger(t_1)] | \Psi_\alpha; \mathbf{q} \lambda \rangle \\
P_{\alpha\beta,4} &= \frac{(-i)^2}{2!\hbar^2} \iiint_{-\infty}^{+\infty} dt_1 dt_2 dt_3 \sum_{\mathbf{k}'_1 \mathbf{k}'_2 \mathbf{q}'_1 \sigma'_1 \sigma'_2} \sum_{\mathbf{k}' \mathbf{q}' \lambda' \sigma'} \frac{1}{2} U(\mathbf{k}'_1, \mathbf{k}'_2, \mathbf{q}'_1; t_2, t_3) g_{\lambda'}(\mathbf{k}', \mathbf{q}') \\
&\quad \times \langle \Psi_\beta; \mathbf{k}_1 \sigma_1, \mathbf{k}_2 \sigma_2 | T_t f_{\mathbf{k}'_1 + \mathbf{q}'_1 \sigma'_1}^\dagger(t_2) d_{\mathbf{k}'_1 \sigma'_1}(t_2) f_{\mathbf{k}'_2 - \mathbf{q}'_1 \sigma'_2}^\dagger(t_3) c_{\mathbf{k}'_2 \sigma'_2}(t_3) d_{\mathbf{k}' + \mathbf{q}' \sigma'}^\dagger(t_1) c_{\mathbf{k}' \sigma'}(t_1) [a_{\mathbf{q}' \lambda'}(t_1) + a_{-\mathbf{q}' \lambda'}^\dagger(t_1)] | \Psi_\alpha; \mathbf{q} \lambda \rangle
\end{aligned} \tag{B4}$$

With similar calculation to $P_{\alpha\beta,1}$, we can show that $P_{\alpha\beta,i}$, $i = 2, 3, 4$ follow Eqs. (13) and (14).

Appendix C: Calculation of $P_{\alpha\beta,i}$, $i = 5, 6, 7, 8$ in type-II photoemission

In this Appendix section, we will calculate the contributions from type-II photoemission to the coincidence detection probability. They are described by $P_{\alpha\beta,i}$, $i = 5, 6, 7, 8$, which are schematically shown in Fig. 3. Mathematically, they are defined as below:

$$\begin{aligned}
P_{\alpha\beta,5} &= \frac{(-i)^2}{2!\hbar^2} \iiint_{-\infty}^{+\infty} dt_1 dt_2 dt_3 \sum_{\mathbf{k}'_1 \mathbf{k}'_2 \mathbf{q}'_1 \sigma'_1 \sigma'_2} \sum_{\mathbf{k}' \mathbf{q}' \lambda' \sigma'} \frac{1}{2} U(\mathbf{k}'_1, \mathbf{k}'_2, \mathbf{q}'_1; t_2, t_3) g_{\lambda'}(\mathbf{k}', \mathbf{q}') \\
&\quad \times \langle \Psi_\beta; \mathbf{k}_1 \sigma_1, \mathbf{k}_2 \sigma_2 | T_t f_{\mathbf{k}'_1 + \mathbf{q}'_1 \sigma'_1}^\dagger(t_2) c_{\mathbf{k}'_1 \sigma'_1}(t_2) d_{\mathbf{k}'_2 - \mathbf{q}'_1 \sigma'_2}^\dagger(t_3) c_{\mathbf{k}'_2 \sigma'_2}(t_3) f_{\mathbf{k}' + \mathbf{q}' \sigma'}^\dagger(t_1) d_{\mathbf{k}' \sigma'}(t_1) [a_{\mathbf{q}' \lambda'}(t_1) + a_{-\mathbf{q}' \lambda'}^\dagger(t_1)] | \Psi_\alpha; \mathbf{q} \lambda \rangle \\
P_{\alpha\beta,6} &= \frac{(-i)^2}{2!\hbar^2} \iiint_{-\infty}^{+\infty} dt_1 dt_2 dt_3 \sum_{\mathbf{k}'_1 \mathbf{k}'_2 \mathbf{q}'_1 \sigma'_1 \sigma'_2} \sum_{\mathbf{k}' \mathbf{q}' \lambda' \sigma'} \frac{1}{2} U(\mathbf{k}'_1, \mathbf{k}'_2, \mathbf{q}'_1; t_2, t_3) g_{\lambda'}(\mathbf{k}', \mathbf{q}') \\
&\quad \times \langle \Psi_\beta; \mathbf{k}_1 \sigma_1, \mathbf{k}_2 \sigma_2 | T_t f_{\mathbf{k}'_1 + \mathbf{q}'_1 \sigma'_1}^\dagger(t_2) c_{\mathbf{k}'_1 \sigma'_1}(t_2) d_{\mathbf{k}'_2 - \mathbf{q}'_1 \sigma'_2}^\dagger(t_3) c_{\mathbf{k}'_2 \sigma'_2}(t_3) f_{\mathbf{k}' + \mathbf{q}' \sigma'}^\dagger(t_1) d_{\mathbf{k}' \sigma'}(t_1) [a_{\mathbf{q}' \lambda'}(t_1) + a_{-\mathbf{q}' \lambda'}^\dagger(t_1)] | \Psi_\alpha; \mathbf{q} \lambda \rangle \\
P_{\alpha\beta,7} &= \frac{(-i)^2}{2!\hbar^2} \iiint_{-\infty}^{+\infty} dt_1 dt_2 dt_3 \sum_{\mathbf{k}'_1 \mathbf{k}'_2 \mathbf{q}'_1 \sigma'_1 \sigma'_2} \sum_{\mathbf{k}' \mathbf{q}' \lambda' \sigma'} \frac{1}{2} U(\mathbf{k}'_1, \mathbf{k}'_2, \mathbf{q}'_1; t_2, t_3) g_{\lambda'}(\mathbf{k}', \mathbf{q}') \\
&\quad \times \langle \Psi_\beta; \mathbf{k}_1 \sigma_1, \mathbf{k}_2 \sigma_2 | T_t d_{\mathbf{k}'_1 + \mathbf{q}'_1 \sigma'_1}^\dagger(t_2) c_{\mathbf{k}'_1 \sigma'_1}(t_2) f_{\mathbf{k}'_2 - \mathbf{q}'_1 \sigma'_2}^\dagger(t_3) c_{\mathbf{k}'_2 \sigma'_2}(t_3) f_{\mathbf{k}' + \mathbf{q}' \sigma'}^\dagger(t_1) d_{\mathbf{k}' \sigma'}(t_1) [a_{\mathbf{q}' \lambda'}(t_1) + a_{-\mathbf{q}' \lambda'}^\dagger(t_1)] | \Psi_\alpha; \mathbf{q} \lambda \rangle \\
P_{\alpha\beta,8} &= \frac{(-i)^2}{2!\hbar^2} \iiint_{-\infty}^{+\infty} dt_1 dt_2 dt_3 \sum_{\mathbf{k}'_1 \mathbf{k}'_2 \mathbf{q}'_1 \sigma'_1 \sigma'_2} \sum_{\mathbf{k}' \mathbf{q}' \lambda' \sigma'} \frac{1}{2} U(\mathbf{k}'_1, \mathbf{k}'_2, \mathbf{q}'_1; t_2, t_3) g_{\lambda'}(\mathbf{k}', \mathbf{q}') \\
&\quad \times \langle \Psi_\beta; \mathbf{k}_1 \sigma_1, \mathbf{k}_2 \sigma_2 | T_t d_{\mathbf{k}'_1 + \mathbf{q}'_1 \sigma'_1}^\dagger(t_2) c_{\mathbf{k}'_1 \sigma'_1}(t_2) f_{\mathbf{k}'_2 - \mathbf{q}'_1 \sigma'_2}^\dagger(t_3) c_{\mathbf{k}'_2 \sigma'_2}(t_3) f_{\mathbf{k}' + \mathbf{q}' \sigma'}^\dagger(t_1) d_{\mathbf{k}' \sigma'}(t_1) [a_{\mathbf{q}' \lambda'}(t_1) + a_{-\mathbf{q}' \lambda'}^\dagger(t_1)] | \Psi_\alpha; \mathbf{q} \lambda \rangle
\end{aligned}$$

With a similar calculation to type-I photoemission, we can obtain Eqs. (16), (17) and (19).

- Rev. Mod. Phys. **78**, 17 (2006), URL <http://link.aps.org/doi/10.1103/RevModPhys.78.17>.
- [3] E. Fradkin, S. A. Kivelson, M. J. Lawler, J. P. Eisenstein, and A. P. Mackenzie, Annu. Rev. Condens. Matter Phys. **1**, 153 (2010), URL <https://doi.org/10.1146/annurev-conmatphys-070909-103027>.
- [4] G. R. Stewart, Rev. Mod. Phys. **83**, 1589 (2011), URL <http://link.aps.org/doi/10.1103/RevModPhys.83.1589>.
- [5] X. Chen, P. Dai, D. Feng, T. Xiang, and F.-C. Zhang, Natl. Sci. Rev. **1**, 371 (2014), ISSN 2095-5138, URL <https://doi.org/10.1093/nsr/nwu007>.
- [6] Y. Su and C. Zhang, Phys. Rev. B **101**, 205110 (2020), URL <https://link.aps.org/doi/10.1103/PhysRevB.101.205110>.
- [7] Y. Su, S. Wang, and C. Zhang, Phys. Rev. B **103**, 054431 (2021), URL <https://link.aps.org/doi/10.1103/PhysRevB.103.054431>.
- [8] H. W. Haak, G. A. Sawatzky, and T. D. Thomas, Phys. Rev. Lett. **41**, 1825 (1978), URL <https://link.aps.org/doi/10.1103/PhysRevLett.41.1825>.
- [9] T. Weber, H. Giessen, M. Weckenbrock, G. Urbasch, A. Staudte, L. Spielberger, O. Jagutzki, V. Mergel, M. Vollmer, and R. Dörner, Nature (London) **405**, 658 (2005), URL <https://doi.org/10.1038/35015033>.
- [10] W. Vanroose, F. Martin, T. N. Rescigno, and C. William McCurdy, Science **310**, 1787 (2005), URL <https://www.science.org/doi/abs/10.1126/science.1120263>.
- [11] D. Akoury, K. Kreidi, T. Jahnke, T. Weber, A. Staudte, M. Schöffler, N. Neumann, J. Titze, L. P. H. Schmidt, A. Czasch, et al., Science **318**, 949 (2007), URL <https://www.science.org/doi/abs/10.1126/science.1144959>.
- [12] N. Fominykh, J. Berakdar, J. Henk, and P. Bruno, Phys. Rev. Lett. **89**, 086402 (2002), URL <https://link.aps.org/doi/10.1103/PhysRevLett.89.086402>.
- [13] A. Trütschler, M. Huth, C.-T. Chiang, R. Kamrula, F. O. Schumann, J. Kirschner, and W. Widra, Phys. Rev. Lett. **118**, 136401 (2017), URL <https://link.aps.org/doi/10.1103/PhysRevLett.118.136401>.
- [14] Y. Aliaev, I. Kostanovskiy, J. Kirschner, and F. Schumann, Surf. Sci. **677**, 167 (2018), ISSN 0039-6028, URL <https://www.sciencedirect.com/science/article/pii/S0039602818300000>.
- [15] K. A. Kouzakov and J. Berakdar, Phys. Rev. Lett. **91**, 257007 (2003), URL <https://link.aps.org/doi/10.1103/PhysRevLett.91.257007>.
- [16] J. Berakdar, Phys. Rev. B **58**, 9808 (1998), URL <https://link.aps.org/doi/10.1103/PhysRevB.58.9808>.
- [17] N. Fominykh, J. Henk, J. Berakdar, P. Bruno, H. Gollisch, and R. Feder, Solid State Commun. **113**, 665 (2000), ISSN 0038-1098, URL <https://www.sciencedirect.com/science/article/pii/S0038109800000000>.
- [18] Y. Pavlyukh, M. Schüler, and J. Berakdar, Phys. Rev. B **91**, 155116 (2015), URL <https://link.aps.org/doi/10.1103/PhysRevB.91.155116>.
- [19] E. E. Salpeter and H. A. Bethe, Phys. Rev. **84**, 1232 (1951), URL <https://link.aps.org/doi/10.1103/PhysRev.84.1232>.
- [20] M. Gell-Mann and F. Low, Phys. Rev. **84**, 350 (1951), URL <https://link.aps.org/doi/10.1103/PhysRev.84.350>.
- [21] A. Damascelli, Z. Hussain, and Z.-X. Shen, Rev. Mod. Phys. **75**, 473 (2003), URL <https://link.aps.org/doi/10.1103/RevModPhys.75.473>.
- [22] P. W. Anderson, Phys. Rev. **112**, 1900 (1958), URL <http://link.aps.org/doi/10.1103/PhysRev.112.1900>.
- [23] J. W. Negele and H. Orland, *Quantum many-particle systems* (Addison-Wesley Publishing Company, 1987), ISBN 0-201-12593-5.
- [24] P. B. Littlewood and C. M. Varma, Phys. Rev. Lett. **47**, 811 (1981), URL <http://link.aps.org/doi/10.1103/PhysRevLett.47.811>.
- [25] P. B. Littlewood and C. M. Varma, Phys. Rev. B **26**, 4883 (1982), URL <http://link.aps.org/doi/10.1103/PhysRevB.26.4883>.
- [26] H. Bruus and K. Flensberg, *Introduction to Many-body quantum theory in condensed matter physics*, Oxford Graduate Texts (Oxford University Press, USA, 2002), ISBN 9780198566335.